Joint International Topical Meeting on Mathematics & Computation and Supercomputing in Nuclear Applications (M&C + SNA 2007)
Monterey, California, April 15-19, 2007, on CD-ROM, American Nuclear Society, LaGrange Park, IL (2007)

USING HOMOGENIZED MACROSCOPIC GROUP CROSS SECTIONS IN CONTINUOUS-ENERGY MONTE CARLO NEUTRON TRANSPORT CALCULATIONS WITH MCNP

J.C. Kuijper, S.C. van der Marck and A. Hogenbirk
NRG
Westerduinweg 3, P.O. Box 25, NL-1755 ZG Petten, The Netherlands
kuijper@nrg-nl.com; vandermarck@nrg-nl.com

Key Words: MCNP, Macroscopic Group Cross Sections

ABSTRACT

A method has been developed to include diffusion-theory-type (macroscopic) group cross sections into MCNP, while still running in continuous (point-wise) energy calculation mode. A good agreement is observed between results (k_{eff}, reaction rates and flux profiles) from a heterogeneous - reference - MCNP calculation and those from MCNP calculations based on homogenised macroscopic group cross sections, obtained from the heterogeneous MCNP calculation and ELNINJO post-processing. Also a good agreement is observed between results from MCNP transport-theory calculations and PANTHER diffusion-theory calculations, based on exactly the same macroscopic group cross sections, although effects of the fundamental differences between transport- and diffusion theory are apparent as well. The presented results provide further evidence for the validity of the MCNP-ELNINJO method for the generation of homogenised (macroscopic) group cross sections for complicated geometries. Furthermore, the method presented opens the possibility to speed up continuous-energy MCNP calculations, as less important regions of a large, complicated geometry can be replaced by homogenised areas with appropriate group cross sections, while the details of the important sections are retained.

1. INTRODUCTION

Homogenized (macroscopic) group cross sections play an important role in making reactor calculations efficient. As nowadays a detailed 3-D full core calculation combining neutronics, burn-up and thermal hydraulics can still not be considered feasible for routine use, the standard procedure for a 3-D full-core (LWR) calculation (either neutronics only or combined neutronics/thermal hydraulics) is to use an assembly code to calculate sets of macroscopic group cross sections for homogenized (fuel) blocks in the reactor, which are dependant upon quantities such as fuel temperature, moderator density, burn-up, boric acid concentration, etc. In the (usually 2-D) assembly code the geometrical details of the fuel assemblies (and also of the reflector structures) are modelled. The 3-D full core calculations (usually applying nodal diffusion theory) are then performed in a geometry consisting of homogeneous blocks with associated macroscopic cross sections, which have been prepared in such a way that certain neutron interaction and/or leakage rate are preserved, when compared with calculations performed in detailed geometry.

A similar calculation scheme is also employed for the -approximately- monthly cycle analysis/fuel loading pattern design of the High Flux Reactor (HFR) in Petten, The Netherlands. As is described in an earlier paper [1], the full core cycle calculations are performed by the OSCAR-3 3-D nodal diffusion code [2]. The required sets of (macroscopic) broad-group cross sections are either generated by the HEADE module of the OSCAR code system (for the fuel elements) or by the 2-D neutron transport code WIMS [3] (for the in-core and ex-core irradiation experiments and isotope production facilities). A recent development is the use of the 3-D general geometry, continuous energy Monte Carlo N-particle transport code MCNP [4], in combination with the post-processing system ELNINJO [1], to generate effective broad-group cross sections for irradiation experiments and isotope production facilities. Irradiation experiments with strong geometrical and/or material variations in the axial direction can thus be treated in the OSCAR-3 cycle calculation, as well as experiments with very complicated geometries, as long as MCNP models of these experiments are available.

2. WHY USE MACROSCOPIC GROUP CROSS SECTIONS IN MCNP?

For checking purposes also a full 3-D MCNP model of the HFR is available. This model can also be used to study in detail the behaviour of an irradiation experiment interacting with its detailed surroundings, i.e. the HFR. However, when many runs are required, e.g. in the design phase of an experiment, in order to study different options, running a full, detailed 3-D HFR MCNP model requires large computation power and/or a large amount of time.
Therefore some extension modules to the ELNINJO system have been developed which enable the use of macroscopic broad-group (diffusion-theory type) cross sections in MCNP, still running in continuous energy mode. In this way an irradiation experiment can still be modelled in great detail, while the remaining part of the HFR can be modelled as a collection of homogeneous blocks (each with its own set of flux-volume weighted macroscopic group cross sections), hereby preserving the global neutron flux (and power-) distribution and global reactor parameters, such as k_{eff}.

3. IMPLEMENTATION

Introducing broad-group macroscopic cross sections in MCNP, while still running in continuous energy mode, involves the addition of pseudo-nuclides, with piece-wise constant cross sections into the MCNP cross section library, i.e. a histogram-type cross section. If the number of macroscopic cross section sets (one for each homogenized material) is small, it is feasible to generate and add an MCNP pseudo-nuclide to the MCNP library for each of these sets. The corresponding homogeneous block in the geometry is then filled with this pseudo nuclide at unit density. For each of the pseudo nuclides the cross section data to be inserted into the MCNP library has to adhere to the applicable rules for consistency for MCNP libraries.
The self-scatter term, which is not required in diffusion theory, should be chosen in such a way that a set of partial cross sections for a given group adds up to the transport-corrected total cross section. This is a well-known approximation method to implement first-order scattering anisotropy [5].

A description of the continuous energy data format of the MCNP ACE-type data libraries is given in [6]. As mentioned in the previous section a set of macroscopic diffusion-theory-type cross sections will be represented by a pseudo nuclide. A typical set of diffusion-theory-type macroscopic G-group cross sections for a homogenised material consists of:

- macroscopic transport corrected total cross section $\Sigma_{tr}^{(g)}$ (or diffusion coefficient $D^{(g)}$; g = 1,...,G)); generally $D^{(g)} = (3\ \Sigma_{tr}^{(g)})^{-1}$;
- macroscopic absorption cross section $\Sigma_a^{(g)}$;
- macroscopic (n,2n) cross section $\Sigma_{n,2n}^{(g)}$;
- macroscopic fission cross section $\Sigma_f^{(g)}$;
- group-dependent fission neutron yield $\nu^{(g)}$;
- fission spectrum $\chi^{(g)}$;
- macroscopic (isotropic) scatter matrix $\Sigma_s^{(g\rightarrow g')}$ ($g \neq g'$);

The macroscopic absorption cross section can also be regarded as the sum of the:

- macroscopic fission cross section $\Sigma_f^{(g)}$, and the
- macroscopic capture cross section $\Sigma_c^{(g)}$.

Generally, the macroscopic transport corrected total cross section (in brief: transport cross section) is given by:

$$\Sigma_{tr}^{(g)} = \Sigma_{tot}^{(g)} - \mu^{(g)}\ \Sigma_s^{(g\rightarrow g)} \tag{1}$$

with $\mu^{(g)}$ the average cosine of the scattering angle (LAB system) in group g.
Diffusion-theory-type macroscopic cross section data, as described above, can be converted into the MCNP/Ace continuous-energy format by applying a set of conversion rules. In this conversion it is assumed that the scattering matrix is isotropic. First-order anisotropic effects are assumed to be taken into account in the transport-corrected total cross section or "transport cross section" [5], which is to be used instead of the total cross section. For this the (isotropic) self-scatter cross section $\Sigma_s^{(g\rightarrow g)}$, which is not used in neutron diffusion theory, has to be adapted in such a way that:

$$\Sigma_{tr}^{(g)} = \Sigma_a^{(g)} + \Sigma_{n,2n}^{(g)} + \sum_{g \neq g'} \Sigma_s^{(g\rightarrow g')} + \Sigma_s^{(g\rightarrow g)} \tag{2}$$

or:

$$\Sigma_S^{(g\rightarrow g)} = \Sigma_{tr}^{(g)} - \Sigma_{n,2n}^{(g)} - \sum_{g \neq g'} \Sigma_s^{(g\rightarrow g')} - \Sigma_a^{(g)} \tag{3}$$

For the (n,2n) cross section it is further assumed that the outgoing neutrons are in the same energy group as the incoming neutron, with isotropic angular distribution. This leads to the correspondence between MCNP/Ace-type cross sections and diffusion-theory-type microscopic cross sections, as listed in Table I. The elastic and inelastic scattering are summed and represented as MT4 (inelastic scattering), because MCNP would use, at the microscopic level, the correlation between the incoming and outgoing energies and angles, which is undesirable in this case as this type of information is already included, to the extent possible, in the transport cross section.

Table I. Conversion of macroscopic diffusion-theory-type cross sections into MCNP/Ace continuous energy format.

Diffusion theory macro cross section	MCNP/Ace cross section	MT	Value	Remarks
Transport	Total	1	$\Sigma_{tr}^{(g)}/\sigma_0$	(MT1000/ 1001)
-	Elastic	2	0	
Scatter	Non-elastic	4	$\Sigma_s^{(g\rightarrow g')}/\sigma_0$	All scatter into non-elastic
Capture	Capture	101	$\Sigma_c^{(g)}/\sigma_0$	
n.2n	n,2n	16	$\Sigma_{n,2n}^{(g)}/\sigma_0$	
Fission	Fission	18	$\Sigma_f^{(g)}/\sigma_0$	
Fission neutron yield	Fission neutron yield	452	$\nu^{(g)}$	
Fission spectrum	Fission spectrum	1018	$\chi^{(g')}$	g' is energy group of outgoing neutron

It should be noted that some additional data has to be provided, viz. the unit microscopic cross section σ_0 (e.g. 1 barn) and the mass A of the pseudo nuclide to be added to the MCNP/Ace library. Any influence of the nuclide mass A on the kinematics in MCNP should be eliminated by setting the temperature of the material to zero (or, in practice, a very small number, e.g. 1E-20) in the MCNP input deck. It should also be noted that the group cross sections (and the energy distribution of outgoing neutrons) have to be implemented as histograms in the continuous energy MCNP/Ace format.. This can be done by using the e.g. extension ".04d" (for discrete data) instead of ".04c" (for continuous energy data) [4]. A correct choice of interpolation scheme ensures that the data are used as histograms (ENDF interpolation type 1, see Ref. [7]). In the implementation in an MCNP/Ace library, the energy distribution of the outgoing neutrons is expected in the form of a probability density function, which yields 1 when integrated over the energy.

Finally, it should be noted that the actual source of the broad-group macroscopic group cross sections may be either MCNP/ELNINJO or OSCAR-3/HEADE, or WIMS or any other deterministic or Monte Carlo (macroscopic) cross section calculation scheme.

Table II. Energy group structure used in this study.

Energy group	Upper energy boundary
1	20 MeV
2	0.821 MeV
3	5.53 keV
4	4.00 eV
5	0.625 eV
6	0.25 eV
7	0.058 eV

Table III. The mean free path per energy group, estimated as $1/\Sigma_{tr}$.

Energy	Fuel zone		Water zone	
Group	OUTscatter	INscatter	OUTscatter	INscatter
1	9.78 cm	8.10 cm	10.85 cm	7.90 cm
2	3.97 cm	3.91 cm	3.77 cm	3.54 cm
3	3.27 cm	3.38 cm	2.45 cm	2.45 cm
4	2.73 cm	3.10 cm	2.01 cm	2.32 cm
5	1.86 cm	2.22 cm	1.45 cm	1.72 cm
6	1.10 cm	1.14 cm	0.81 cm	0.82 cm
7	0.60 cm	0.60 cm	0.45 cm	0.45 cm
total	2.85 cm	2.85 cm	0.93 cm	0.93 cm

Table IV. Results for k_{eff} using different methods and codes.

Model	MCNP	PANTHER
Detailed model	1.48286 ± 0.00176	
No transport correction	1.46215 ± 0.00043	
Inscatter approximation	1.48902 ± 0.00040	1.49063
Outscatter approximation	1.48597 ± 0.00037	1.48703

4. DEMONSTRATION

In order to demonstrate the feasibility of the use in MCNP of macroscopic group cross sections for homogenized materials, possibly in combination with a detailed description of other parts of the geometry (and point-energy microscopic cross sections), a relatively simple, but nevertheless demanding (one-dimensional) model was defined, based upon de combination of an HFR fuel element, consisting of a series of fuel plates, adjacent to an empty core position filled with water (see Fig. 1). Reflective boundary conditions are assumed on each of the six outer boundaries of the model. The dimensions of this simplified "HFR fuel element/water section"-combination correspond to the actual dimensions in the HFR, perpendicular to the fuel plates. Fig. 2 demonstrates the simplicity of the MCNP input deck for the homogenised model. The same model was also implemented in the 3-D nodal diffusion-theory code PANTHER [8].
Employing MCNP and the ELNINJO post-processing system, diffusion-theory-type macroscopic cross sections in 7 energy groups (see Table II) were calculated for the fuel section ("Pseudo Isotope 1") and the water section ("Pseudo Isotope 2"). As ELNINJO offers 3 possibilities for the calculation of the transport section, viz. "inscatter" approximation, "outscatter" approximation

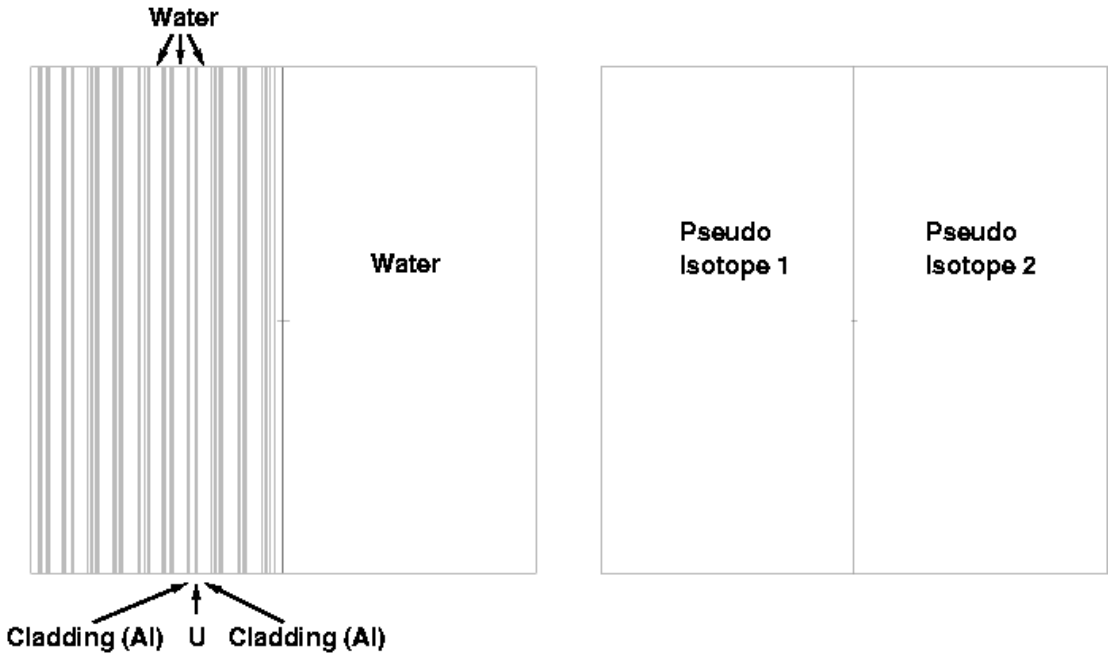

Figure 1. The detailed model (left) and the homogenised model (right) of half a fuel position and half a water position in the HFR, with reflecting boundaries on all sides.

```
model using homogenized group cross sections
  1  1  0.01     1  -2     3  -4     6  -7   tmp=1e-20  imp:n=1
  2  2  0.01     1  -2     4  -5     6  -7   tmp=1e-20  imp:n=1
  3  0          -1 : 2 : -3 : 5 : -6 : 7              imp:n=0

   *1  px      -3.855
   *2  px       3.855
   *3  py       0
    4  py       4.05
   *5  py       8.1
   *6  pz      -6.0
   *7  pz       6.0

  kcode    1000 1.3  10  500
  ksrc     0 2 0
  m1   999001.04d  1
  m2   999002.04d  1
```

Figure 2. The input deck for the simplified (homogenised 2-zone) MCNP model.

[5] and no correction at all, 3 respective sets of macroscopic group cross sections were calculated. In Table III it is shown that the macroscopic transport cross section values are slightly different for inscatter and outscatter approximation. These differences are also reflected in the results of k_{eff}-calculations, as is demonstrated in Table IV. Regarding the values calculated, by MCNP, for the "Detailed model" as the reference, it is clear that the values calculated by MCNP

for the homogenised model, on the basis of macroscopic cross section data in both the inscatter and outscatter approximation, show a better agreement with the reference than the value calculated without the transport correction.

Table V. The ratio of reaction rates calculated with homogenised group cross sections, using the inscatter approximation, divided by those calculated with the detailed model and point-wise cross sections.

	Fuel zone			Water zone		
group	mt=2	mt=18	mt=101	mt=2	mt=18	mt=101
1	0.839	1.001	1.001	0.829	_	0.982
2	0.671	0.997	0.997	0.685	_	0.984
3	0.477	1.014	1.014	0.456	_	0.971
4	0.435	1.019	1.019	0.389	_	0.978
5	0.417	1.022	1.022	0.380	_	0.979
6	0.547	1.021	1.022	0.441	_	0.988
7	0.684	0.996	0.996	0.658	_	0.993
total	0.587	1.003	1.006	0.707	_	0.982

Table VI. The ratio of reaction rates calculated, by MCNP, with homogenised group cross sections, using the outscatter approximation, divided by those calculated with the detailed model and point-wise cross sections.

	Fuel zone			Water zone		
group	mt=2	mt=18	mt=101	mt=2	mt=18	mt=101
1	0.837	1.001	1.001	0.834	_	0.989
2	0.697	0.993	0.993	0.700	_	0.991
3	0.583	1.008	1.008	0.546	_	0.977
4	0.496	1.014	1.014	0.451	_	0.982
5	0.430	1.019	1.019	0.382	_	0.982
6	0.536	1.015	1.016	0.416	_	0.992
7	0.559	0.985	0.985	0.485	_	1.006
total	0.585	1.001	1.003	0.712	_	0.990

Table VII. The ratio of reaction rates calculated, by MCNP, with homogenised group cross sections, without transport correction, divided by those calculated with the detailed model and point-wise cross sections.

	Fuel zone			Water zone		
group	mt=2	mt=18	mt=101	mt=2	Mt=18	mt=101
1	0.967	0.967	0.967	1.040	_	1.040
2	0.965	0.965	0.965	1.038	_	1.038
3	1.046	1.046	1.046	0.945	_	0.945
4	1.066	1.066	1.066	0.939	_	0.939
5	1.089	1.089	1.089	0.931	_	0.931
6	1.093	1.094	1.095	0.925	_	0.932
7	1.071	1.017	1.017	0.969	_	0.968
total	1.048	0.984	1.000	1.016	_	1.036

This can also be seen in Tables V - VII, which compare group-wise, volume-integrated reaction rates in the fuel and water sections. Note that for the transport-corrected cases (Tables V and VI) the calculated fission (mt = 18) and capture (mt = 101) reaction rates agree very well with the reference, which is most important for the accurate prediction of k_{eff} in this case. For the scatter reaction rate a larger discrepancy is observed, which is expected as the self-scatter cross section has been adjusted as part of the transport correction procedure.
A further comparison between MCNP results, viz. group flux profiles for the heterogeneous (reference) and homogenised models, is shown in Fig. 3. In the fuel section (on the left hand side) the differences are somewhat more pronounced (up to about 10 %), which can be expected due to the heterogeneous nature (fuel plates) of the fuel section in the reference case. In the water section (on the right hand side), which actually *is* homogeneous, the results from both models agree very well indeed. This also provides further evidence that the MCNP-ELNINJO method [1] for the generation of (macroscopic) group cross sections is valid.
Up till now the calculations for the heterogeneous (reference) and homogenised geometries were performed using MCNP, so essentially applying transport theory, although the calculations for the homogenised geometry were based on diffusion-theory-type macroscopic group cross sections. As mentioned earlier, the same homogenised geometry was also modelled in a real diffusion code, viz. the 3-D nodal diffusion code PANTHER [8]. In Table IV it is also shown that the values for k_{eff}, as calculated by the PANTHER code, agree very well with those calculated by MCNP, based on exactly the same macroscopic group cross section data. Fig. 4 presents an intercomparison of the group flux profiles obtained by PANTHER and MCNP. The largest differences, up to 20 %, occur for the 2 highest energy groups (1 and 2). This can be expected, as for these energies a real diffusion-theory-type calculation can not be expected to be able to represent the steep flux gradient at the material interface (at 4.05 cm) occurring in the transport-theory (MCNP) results. For the lower energy groups the flux profiles agree very well.
In Fig. 5 a similar comparison is shown, based on the same data, however for a 10 times enlarged geometry. The largest difference between diffusion and transport theory results occur near the material interface (at 40.5 cm) and deep in the water section, far away from the fuel section. The latter represents a kind of “deep penetration” problem, in which flux anisotropy can be expected to be significant, so that the validity of diffusion theory is highly questionable in that area. However, for the prediction of the k_{eff} and the volume-averaged reaction rates that area is of minor importance as the flux is relatively low.
Finally, it should be noted that no special corrections, like e.g. discontinuity factors, have been applied to obtain a further improvement of the agreement between diffusion and transport theory results.

5. CONCLUSIONS

A method has been presented to incorporate diffusion-theory-type (macroscopic) cross sections into MCNP, while still running in continuous (point-wise) energy calculation mode. A good agreement has been demonstrated between results from a heterogeneous - reference - MCNP calculation and those from MCNP calculations based on homogenised macroscopic group cross sections, obtained from the heterogeneous MCNP calculation and subsequent ELNINJO post-processing.
Also a good agreement was found between results from MCNP transport-theory calculations and PANTHER diffusion-theory calculations, based on exactly the same macroscopic group cross

sections. However, some differences were also observed, due to the fundamental differences between transport- and diffusion theory. Further improvement of the agreement, if required, can be expected from the application of more advanced correction factors, e.g. discontinuity factors.
The presented results provide further evidence for the validity of the MCNP-ELNINJO method for the generation of homogenised (macroscopic) group cross sections for complicated geometries.
Furthermore, the method presented opens the possibility to speed up continuous-energy MCNP calculations, as less important regions of a large, complicated geometry can be replaced by homogenised areas with appropriate group cross sections, while the details of the important section are retained.

REFERENCES

1. S.C. van der Marck, J.C. Kuijper and J. Oppe, ”Homogenized Group Cross Sections by Monte Carlo”, *Proceedings of PHYSOR-2006, ANS Topical Meeting on Reactor Physics*, Vancouver, BC, Canada, September 10 - 14 (2006).
2. E.Z. Müller et al., “Development of a Core Follow Calculational System for Research Reactors”, *Proceedings of the 9th Pacific Basin Nuclear Conference*, Sydney, Australia, May 1 - 6 (1994).
3. “WIMS – a modular system for neutronics calculations – user guide for version 8”, AEA Technology – Nuclear Services, ANSWERS/WIMS(99)9.
4. J.F. Briesmeister (Ed.), “MCNP - A General Monte Carlo N-Particle Transport Code, version 4C”, Report LA-13709-M, Los Alamos National Laboratory, April (2000).
5. R.J.J. Stammler and M.J. Abate, “Methods of Steady-State Reactor Physics in Nuclear Design” (1983).
6. A. Hogenbirk, “Voorgestelde berekeningsmethode van scatter matrix m.b.v. MCNP-ELNINJO”, NRG note 21673/06.73739 FAI/AH/MB, 10. May (2006).
7. V. McLane (Ed.), “Data formats and procedures for the evaluated nuclear data file ENDF-6”, ENDF-102, Brookhaven National Laboratory (1990).
8. P.K. Hutt *et al.*, “The UK Core Performance Package”, Nuclear Energy, J. British Nuclear Energy Society 30, No. 5, p. 291 (1991).

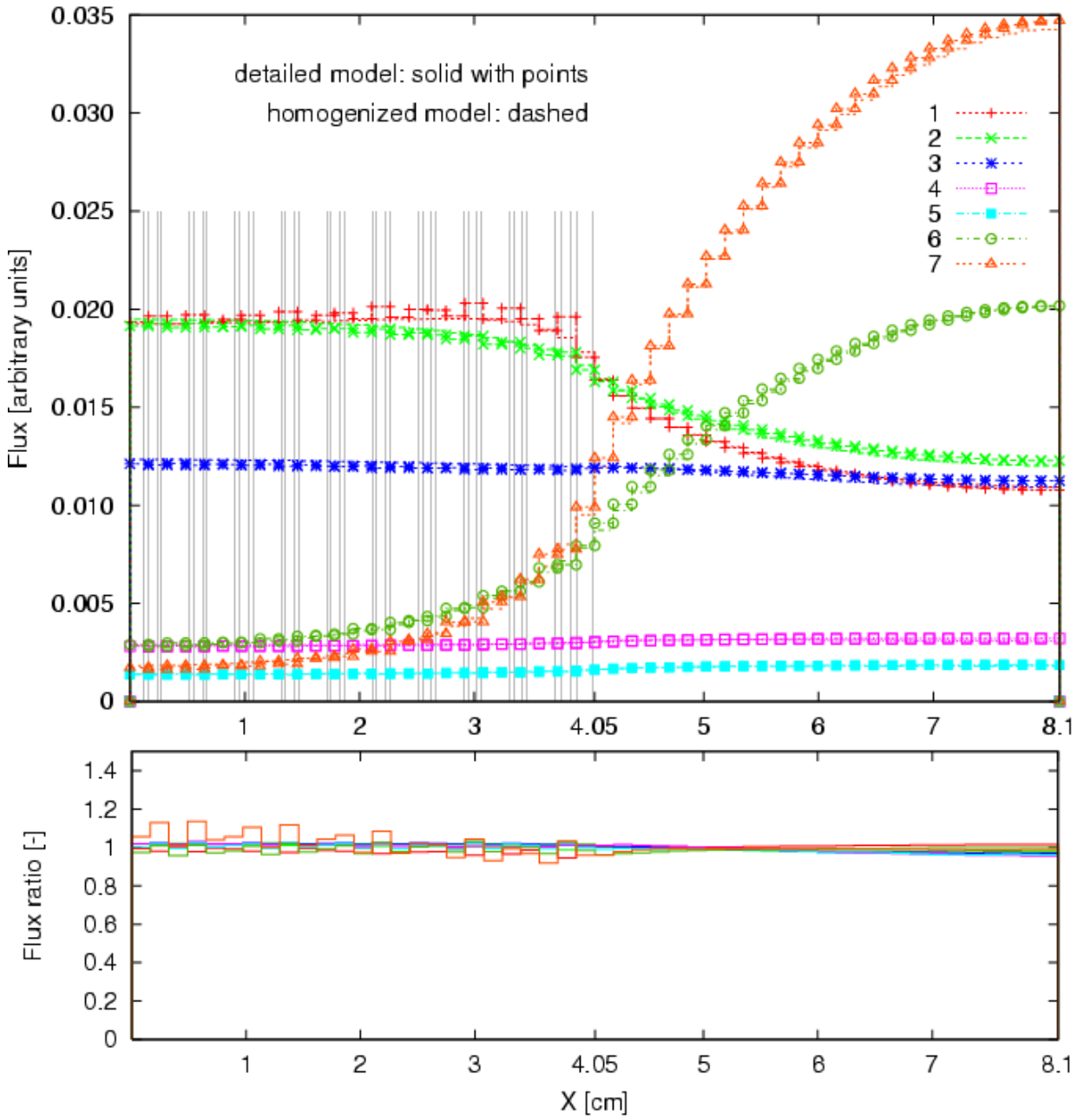

Figure 3. The flux calculated with the detailed MCNP model compared to the flux calculated with the homogenised group cross sections.

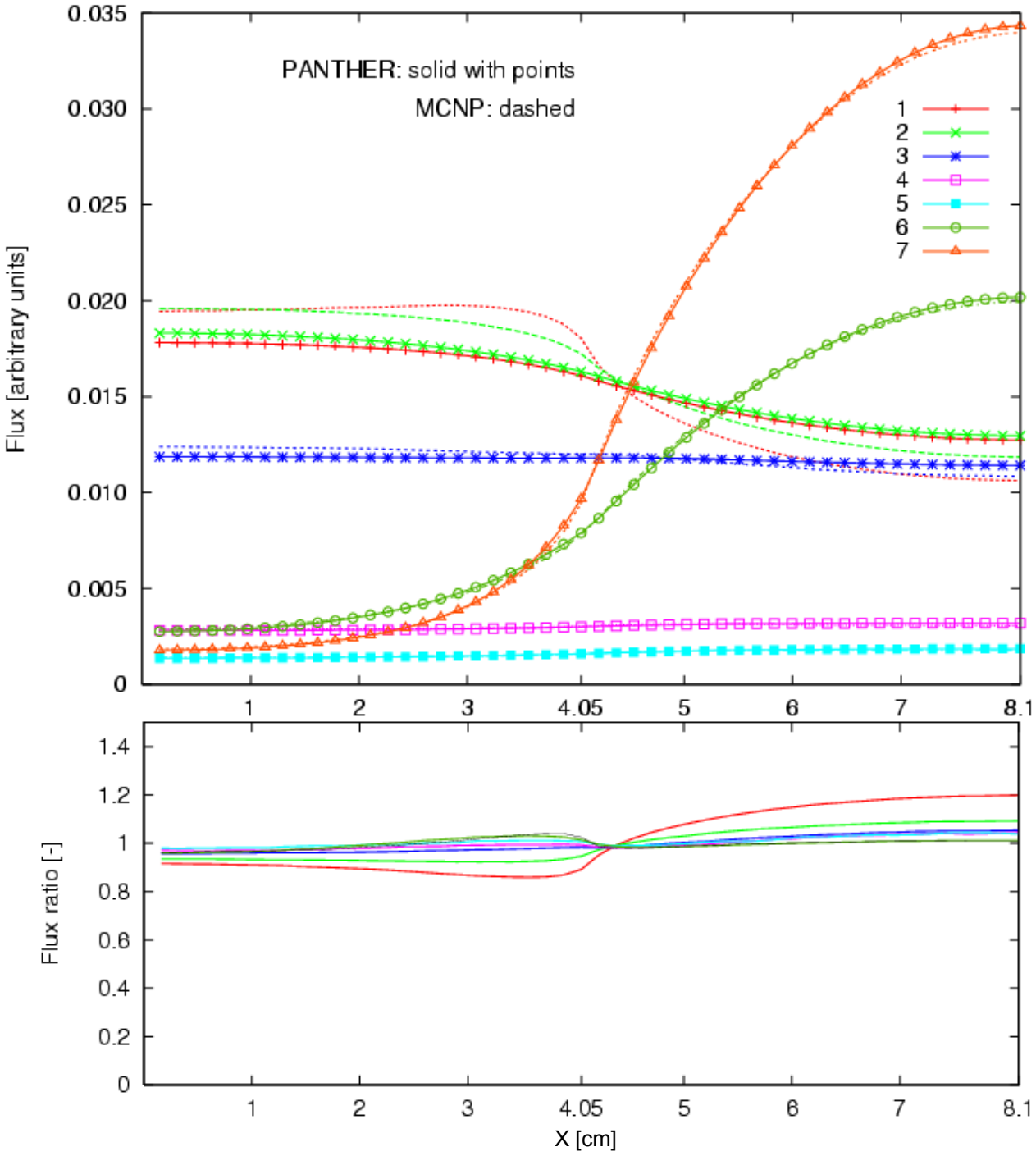

Figure 4. Comparison of group fluxes in HFR-like geometry, as calculated by MCNP (monte carlo transport theory) and PANTHER (diffusion theory), based upon the same set of macroscopic group cross sections for the homogenised fuel and water zones.

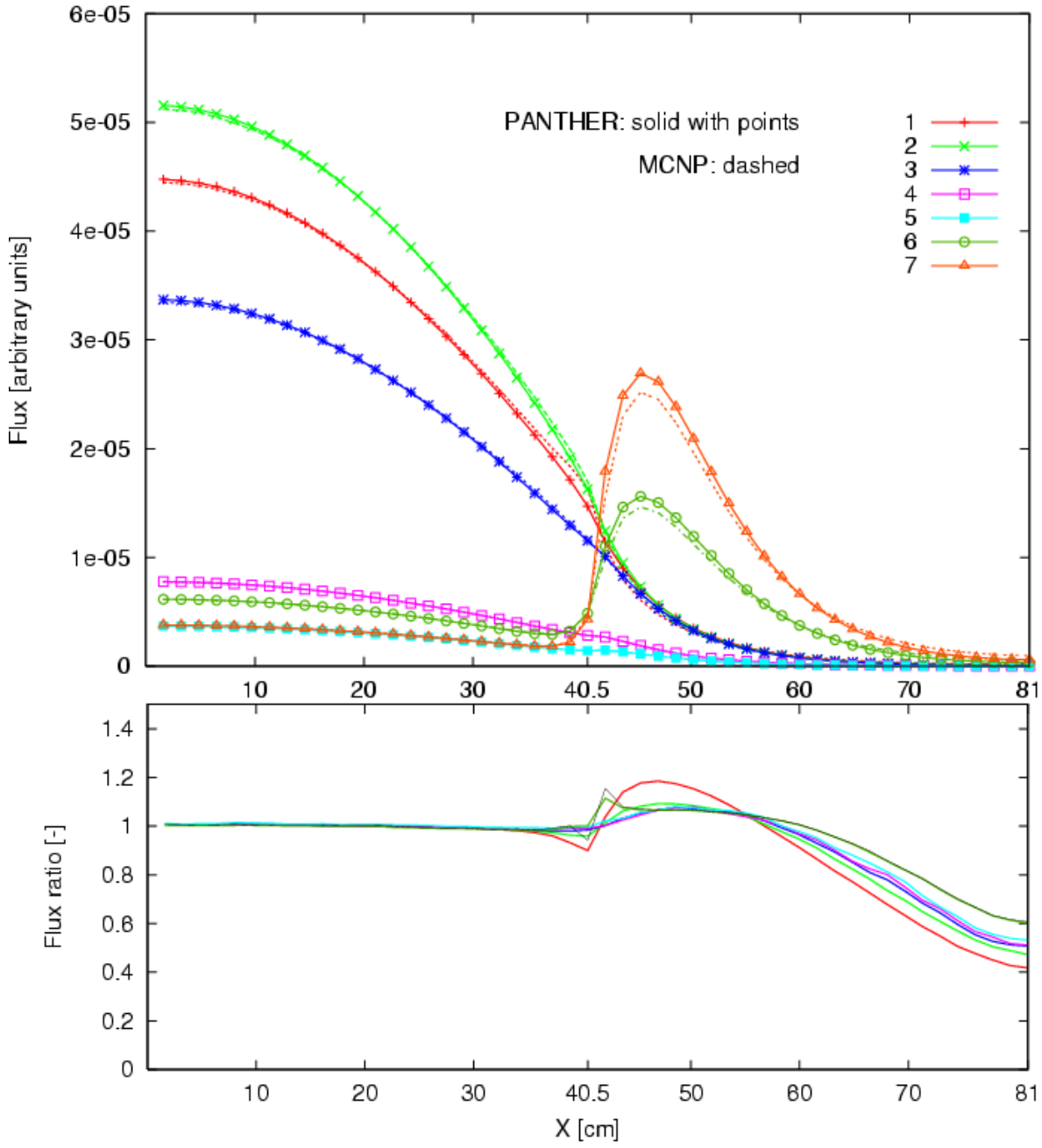

Figure 5. Comparison of group fluxes in 10x enlarged HFR-like geometry, as calculated by MCNP (monte carlo transport theory) and PANTHER (diffusion theory), based upon the same set of macroscopic group cross sections for the homogenised fuel and water zones.